Optical properties and phase-matching in $LiInS_2$

Jinzhe Huang (黄金哲)[1], Deming Ren (任德明)[1], Xiaoyong Hu (胡孝勇)[1], Yanchen Qu (曲彦臣)[1]
Yuri Andreev[2], Pavel Geiko[2], Anna Shaiduko[2], and Sergey Grechin[3]

[1] *Institute of Opto-Electronics, Harbin Institute of Technology, Harbin, 150001*
[2] *Institute of Optical Monitoring SB RAS, Tomsk 634055, Russia*
[3] *SRIRL, Bauman Moscow State Technical University, Moscow 107005, Russia*

Received November 12, 2002

Investigation results on linear and non-linear optical properties, damage threshold and potential efficiencies of biaxial negative $LiInS_2$ crystal are represented. It shows that the crystal has phase-matching and group-velocity matching in wide spectral range for second harmonic, sum- and difference-frequency generation of visible, near and middle IR lasers. The possibilities of designing middle IR optical parametric oscillator (OPO) pumped by Nd:YAG and dye lasers and specially possibility of frequency conversion with 3 μm range femtosecond erbium lasers are given.

OCIS codes: 190.4400, 190.4410, 190.7070.

Biaxial nonlinear crystal $LiInS_2$ with 3.5 g/cm^3 density and 880 °C melting temperature, $3-4$ hardness in Moohs belongs to $mm2$ point group symmetry with $n_x < n_y < n_z$, and is not hygroscopic. Despite of wide transparency spectrum range, rather high coefficient of second order nonlinear susceptibility, relatively high thermal conductivity: 60, 60, and 76 mW/(cm·K) for X, Y, Z crystallooptical axes, and satisfactory birefringence, this crystal, known from 1965[1], attracted little attention in nonlinear optics[1−6]. Conceding to oxide crystals in visible and near IR ranges for damage thresholds, and to many known middle IR crystals of coefficient of second order nonlinear susceptibility, it cannot pretend for a leading position in any part of the spectrum as frequency converter. The difficulties in growing acceptable size high quality crystals were the additional constraining factor. Previously these factors did not allow to determine its optical properties and phase-matching in details, say nothing to experimentally estimate advantages presented by light Li cations or any disadvantages. However, the technological progress stimulate and allow to study optical properties of that crystal in details, and to determine it's potential role and place in nonlinear optics in visible, near and middle IR spectral ranges, and this is the target of our work.

In our research, several transparent or slightly yellowish near $4\times4\times4$ mm^3-sized crystals with rather high optical quality are investigated. The crystals have been grown by the Bridgman-Stockbarger technique. Their transparency ranges are investigated with Shimadzu UV 3101PC (within 0.3−3.2 μm) and Specord 80M (2.5−25.0 μm) spectrophotometers. For example, transparency range of one 3.6-mm-thick colorless crystal is determined as $0.4-12.5$ μm at 0.1 level, and $0.5-9.4$ μm at 0.5 level (Fig. 1(a)).

The transparency is invariable for various polarizations. Long wavelength end can be determined as close to 13.2 μm at 0.1 levels for different samples. At the maximal transparency range of $1.0-8.0$ μm, coefficients of optical losses of $\alpha = 0.1-0.25$ and $\alpha = 1.1-2.3$ cm^{-1} at CO_2 laser wavelengths are obtained. This result is close to the previous one[2], where short-wavelength end of the transmission spectrum of the 3.5-mm-thick crystal with comparable structure and quality is determined as 330 nm at 80 K and 342 nm at 300 K at $\alpha = 200$ cm^{-1} level.

Wavelength dependencies of refraction indices are determined for spectral range $0.45-11.5$ μm by standard method with the help of 5-mm-side prisms. Measurement data are fitted by least square method to the Sellmeier equations with type

$$n^2 = A + B/(\lambda^2 - C) - D\lambda^2, \qquad (1)$$

where λ is in μm. In optical coordinate system of the crystal, the differences between measured and fitted refractive indices are $\leq 10^{-3}$. Estimated Sellmeier coefficients are listed in Table 1.

Dispersion curves of $LiInS_2$ crystal are represented

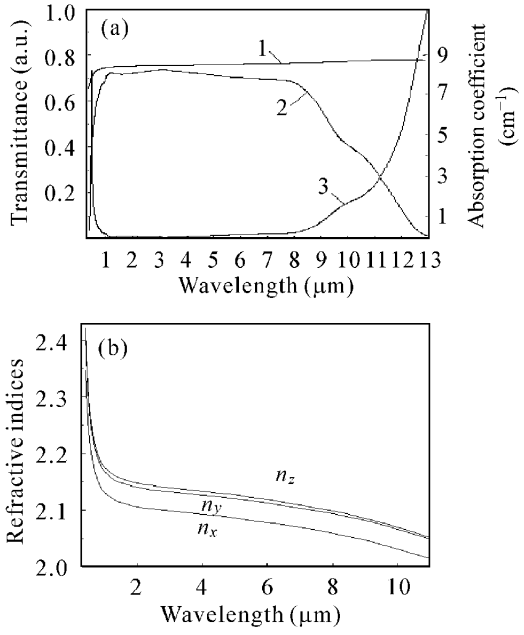

Fig. 1. (a) Fresnel losses (1), transparency spectrum (2), absorption coefficient (3) of 3.6-mm-thick $LiInS_2$, and (b) wavelength dependencies of its refractive indices.

in Fig. 1(b). The main differences between our data on refraction indices and measured in Ref. [1] are not revealed.

It is comfortable to present second harmonic generation (SHG) phase-matching in the form of diagrams. The numbers of transition diagrams between stereographic projections which indicate phase-matching directions in SHG are estimated and given in Table 2 in accordance with the specified classification (digits on the top of first line columns)[4].

These projections show the angle distribution in phase-matching directions for ssf- (solid curves, and the designation of $s-$slow, $f-$fast is accepted here substituting for some expression on $o-$ordinary, $e-$extraordinary) and sff-type interaction (dotted curves). In the projections OZ axis is directed up, OX to the left, and OY orthogonal to figure plane. In conformity to disperse properties of the crystals, the projection view changes (in dependence on different main indices of the refraction coefficients) with laser wavelength variations. Transition wavelengths are specified in the second line of the table. It is seen that, at no wavelength the phase-matching is in the direction of X axis, but SHG phase-matching can take place in wide spectral range of $0.9 - 11.0$ μm. SHG phase-matching diagrams of fsf- and sff-type interaction in XY plane are represented in Fig. 2(a) and spectral bandwidths in Fig. 2(b).

Again we meet with high potential of $LiInS_2$ in SHG with broad spectral bandwidth, which is obviously a good property from practical point of view.

In Fig. 3, OPO phase-matching diagrams of $LiInS_2$ are represented for interactions in volume under Nd:YAG (1.06 μm) pump and for interactions in XY plane under Nd:YAG (1.06 μm), Ho:YLF (2.08 μm) and Er:YAG (2.94 μm) laser pumps.

So, $LiInS_2$ permits design of middle IR OPOs using of all known solid state lasers as pump sources and even is suitable for Nd:YAG second harmonic and dye laser pumps, where two detached curves with the same labeled

Table 1. Sellmeier Coefficients of $LiInS_2$

$LiInS_2$	A	B	C	D
X	4.559534	0.1403701	0.069233	0.0028731
Y	4.418222	0.1254461	0.0657432	0.0028850
Z	4.59206	0.410887	0.069287	0.0030589

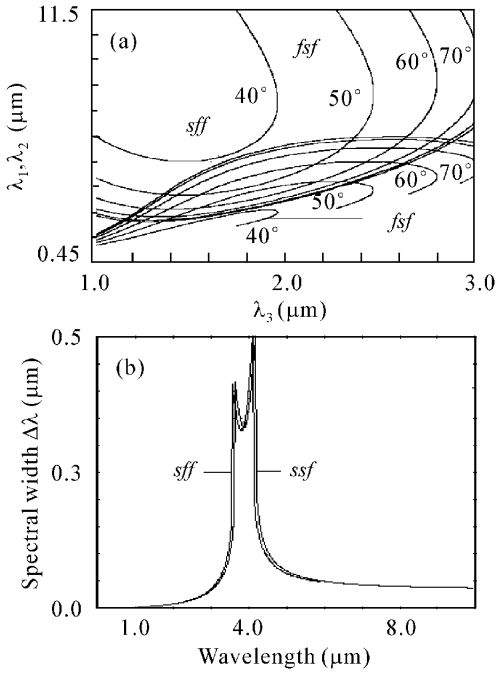

Fig. 2. SHG phase-matching diagrams in XY plane and its spectral bandwidth versus pump wavelength ($\varphi = 0°$).

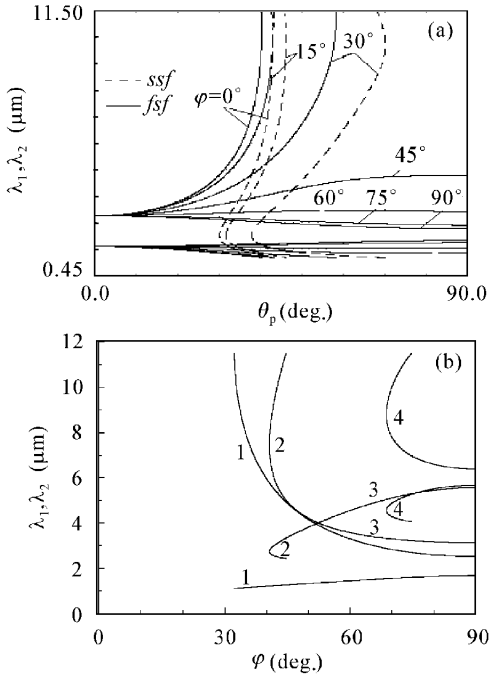

Fig. 3. (a) OPO phase-matching diagrams for ssf- and fsf-type of interaction versus θ angle at different φ values under Nd:YAG pump, and (b) for fsf- (1, 2, 4) and sff-type (3) of interaction in XY plane under Nd:YAG (1), Ho:ILF (2, 3) and Er:YSGG (4) laser pump.

Table 2. The Transitions Between Stereographic Projections of Phase-Matching Directions for SHG

Crystal	Type	00	00-10	10	10-30	30	30-31	31	31-33	33	33-31	31	31-30	30	30-10	10	10-00	00
$LiInS_2$	*ssf*	900	1573.5		1731.9										7945.2		8498.5	11500
	sff						2294.8		2638.3		5104.7		5785.7					

number in Fig. 3(b) denote realizable matching wavelengths λ_1 and λ_2 ($\lambda_1 \geq \lambda_2$), but their interaction subtype (sff) will change through their cross point (to fsf) like curves labeled as 2 (after cross point number 3 is labeled).

It is well known that for efficient frequency conversion of femtosecond pulses, in addition to phase-matching, it has to accommodate group-velocity matching. It means the crystal length must be shorter than so called group length $L_{gr} = \tau/|\Delta u^{-1}|$, where τ is pump pulse duration and

$$\Delta u^{-1} = (1/u_1 - 1/u_2) = 1/c[(n_1 - \lambda_1 \frac{\partial n_1}{\partial \lambda_1}) - (n_2 - \lambda_2 \frac{\partial n_2}{\partial \lambda_2})] \quad (2)$$

is group-velocity mismatch, u_1, u_2, λ_1 and λ_2 are group velocities and wavelengths of pump and second harmonic emissions, respectively. Carrying out simulation confirms that frequency conversion (SHG, sum- and difference frequency generation) of femtosecond pulses can be realized in $LiInS_2$ in wide spectral range. In Fig. 4(a) the dependences of λ_1 and λ_2 on wavelength λ_3 with interactions $\lambda_1 + \lambda_2 \rightarrow \lambda_3$ (before and after cross points are labeled as corresponding numbers indicating concrete interaction types) are submitted for group-velocity matching in XY plane.

Directions of phase- and group-velocity matching at sff-type SHG are shown in Fig. 4(b). The potential use of $LiInS_2$ crystal in frequency conversion of femtosecond pulses includes the realization SHG of femtosecond Er:YSGG (2.79 μm) laser.

Second order nonlinear susceptibility coefficients are determined as $d_{31} = 6.2$, $d_{32} = 5.4$ and $d_{33} = 9.8$ pm/V with accuracy of 15% from comparative measurements of SHG efficiencies in thin wedges (5°) $ZnGeP_2$ on known procedure[1] using Q-switched CO laser. The coefficients $d_{14} = d_{36}$ of $ZnGeP_2$ wedge are accounted as equal to 75 pm/V.

Determined values d_{ij} ($ij = 31, 32, 33$) are about 80% lower than first known data by G. D. Boyd[1] and data by L. Isaenko[5], but are higher than that presented by G. M. H. Knippels[6]. Let us note that for type II interactions, efficient second order nonlinear susceptibility coefficient $d_{\text{eff}} = d_{32} \sin^2 \varphi + d_{31} \cos^2 \varphi$ will be near independent on φ in XY plane provided that the sign of d_{32} to d_{31} are positive.

The above estimations for d_{eff} are carried out in phase-matching directions. But, more information can be obtained by calculating d_{eff} in all possible directions for $LiInS_2$ (φ and θ angles). Correspondent estimations are presented in Fig. 5 in the form of fields of d_{eff} for SHG in the proposal, and both coefficients having same sign.

This representation allows us to find directions of the maximal efficient nonlinearity. It takes place at ssf-type interaction in the direction of Y axis. And it is interesting to note that the position of the maximal efficient nonlinearity is determined for biaxial crystals not only by symmetry group (in nonlinear tensor) but also by relations between tensor components. Due to this reason, the angle distributions of the efficient nonlinearity will be different for crystals belonging to the same $mm2$ point group.

Damage threshold of $LiInS_2$ is determined under identical experimental conditions in comparison with some known and new crystals using the equipment as Ref. [7]. Stable parameters TEA CO_2 laser with ~36 ns FWHM pulses is used in this case. The laser emits pulses with energy $E = 200$ mJ at $9P$ (20) emission line (9.55 μm) with

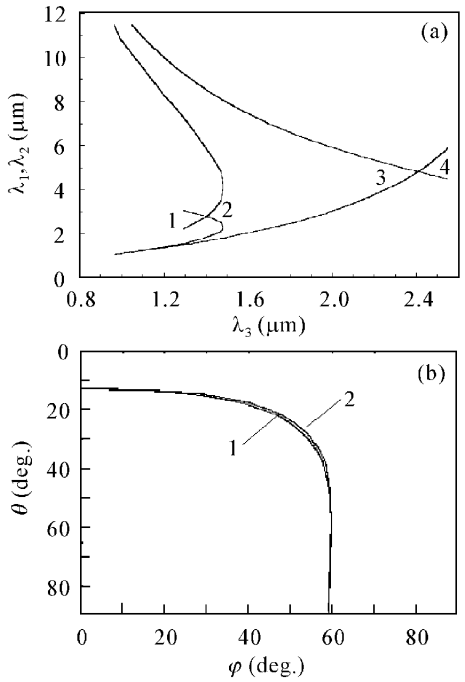

Fig. 4. (a) Spectral dependence of group-velocity matching for ($s_1 - f_3$) (1), ($s_2 - f_3$) (2), ($f_1 - f_3$) (3) and ($f_2 - f_3$)-waves (4) at sff- (1, 4) and fsf-type (2, 3) of interaction in XY plane, and (b) phase- (1) and group-velocity (2) matching directions for ($s_1 - f_3$)-waves at sff-type SHG in $LiInS_2$ volume under 2.8 μm pump.

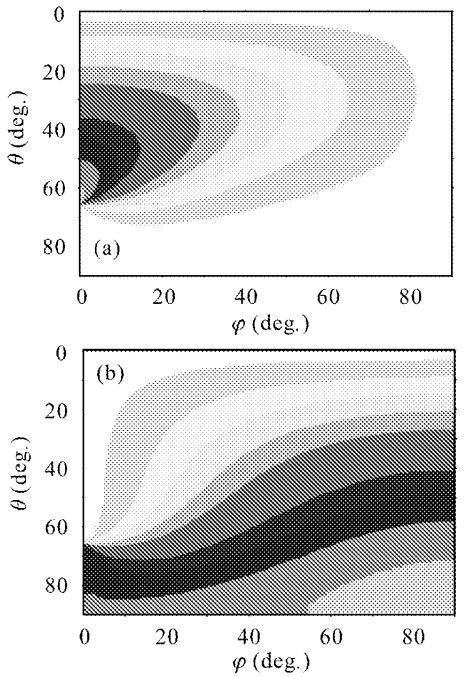

Fig. 5. (a) SHG efficient nonlinearity fields for ssf- (a) and sff-type (b) of interaction.

about 90% energy in leading peak and only ~10% in low intensity pulse's "tails". Total energy variation is not higher than 3.5%, but energy variation in leading peak is not higher than 2% and ±2 ns in its duration. It is determined that the damage threshold 214 MW/cm^2 of $LiInS_2$ is about 1.5 times higher than known crystals such as $CdGeAs_2$ (157 MW/cm^2), $ZnGeP_2$ (142) and $AgGaSe_2$ (139). Up to date, performance on SHG of $2.75-6.0$ μm tunable picosecond free electron laser was obtained[6]. No damage was observed for peak power density of higher than 6 GW/cm^2 at 25 MHz repetition rates of 0.5 ps pulses in that experiment.

To check determined data on optical properties of $LiInS_2$, experiment on SHG of line tunable Q-switched low pressure CO laser is carried out. Measured and estimated phase-matching angles are coincided with accuracy not worse than 0.3°.

In conclusion, linear and nonlinear properties and phase-matching in single $LiInS_2$ crystal are investigated in details, and the damage threshold under the TEA CO_2 laser pump is compared with known crystals under the identical experimental conditions. Investigation results show that $LiInS_2$ is the most prospective crystal for frequency conversion of available near IR femtosecond solid state Ti:sapphire ($0.7-1.1$ μm), Nd:YAG (1.06 μm) and Cr:forsterite ($1.25-1.32$ μm) lasers into middle IR range. It is also the only known crystal suitable for frequency conversion of 3 μm femtosecond erbium lasers. This crystal is also attractive for frequency conversion of visible lasers into the middle IR. Relatively low second order nonlinear susceptibility coefficient is significantly compensated by 1.5 times higher damage threshold, lower refractive indices and rich possibilities to optimize phase-matching in comparison with wide used crystals transparent at visible to middle IR spectral range, such as $AgGaS_2$ or BANAN. Correctness of determined data is confirmed by experimental data on SHG of Q-switched CO laser.

This work was supported by the National Natural Science Foundation of China under Grant No. 69878005 and Natural Science Foundation of Heilongjiang Province under Grant No. F01-10. J. Huang's e-mail address is huang_yin@sohu.com.

References

1. G. D. Boyd, H. M. Kasper, and J. H. McFee, J. Appl. Phys. Lett. **44,** 2808 (1973).
2. T. J. Negran, H. M. Kasper, and A. M. Glass, Mat. Res. Bull. **8,** 743 (1973).
3. T. Kamijoh and K. Kuriyama, J. Cryst. Growth **46,** 801 (1979).
4. S. G. Grechin, S. S. Grechin, and V. G. Dmitriev, Kvantovaya Electronika (in Russian) **30,** 377 (2000).
5. L. Isaenko, I. Vasilieva, A. Yelisseyev, S. Lobanov, V. Malakhov, L. Dovlitova, J.-J. Zondy, and I. Kavun, J. Cryst. Growth **218,** 313 (2000).
6. G. M. H. Knippels, A. F.G. van der Meer, A. M. MacLeod, A. Yelisseyev, L. Isaenko, S. Lobanov, I. Thénot, and J.-J. Zondy, Opt. Lett. **26,** 617 (2001).
7. Y. M. Andreev, V. V. Badikov, V. G. Voevodin, L. G. Geiko, P. P. Geiko, M. V. Ivashchenko, A. I. Karapuzikov, and I. V. Sherstov, Quantum Electron. **31,** 1075 (2001).